Supporting Information for:

Ultra-small iridium oxide nanoparticles: from one-pot hydrothermal synthesis to oxygen evolution reaction catalyst

Laura G. Graversen,[a] Nicolas Schlegel,[a] Freja B. Holde,[a] Adrian S. Arjona,[a] Stefanie Punke,[a] Tobias M. Nielsen,[a] Andy S. Anker,[a] Jonas Forner,[b] Gustav K. H. Wiberg,[b] Matthias Arenz,[b] Rebecca K. Pittkowski,*[,a] and Kirsten M. Ø. Jensen*[,a]

[a] Department of Chemistry and Nanoscience Center, University of Copenhagen, 2100 Copenhagen Ø, Denmark
[b] Department of Chemistry, Biochemistry and Pharmaceutical Sciences, University of Bern, Freiestrasse 3, Bern, 3012, Switzerland
* Corresponding authors: rebecca.pittkowski@chem.ku.dk and Kirsten@chem.ku.dk

Table of Contents

Transmission electron microscopy

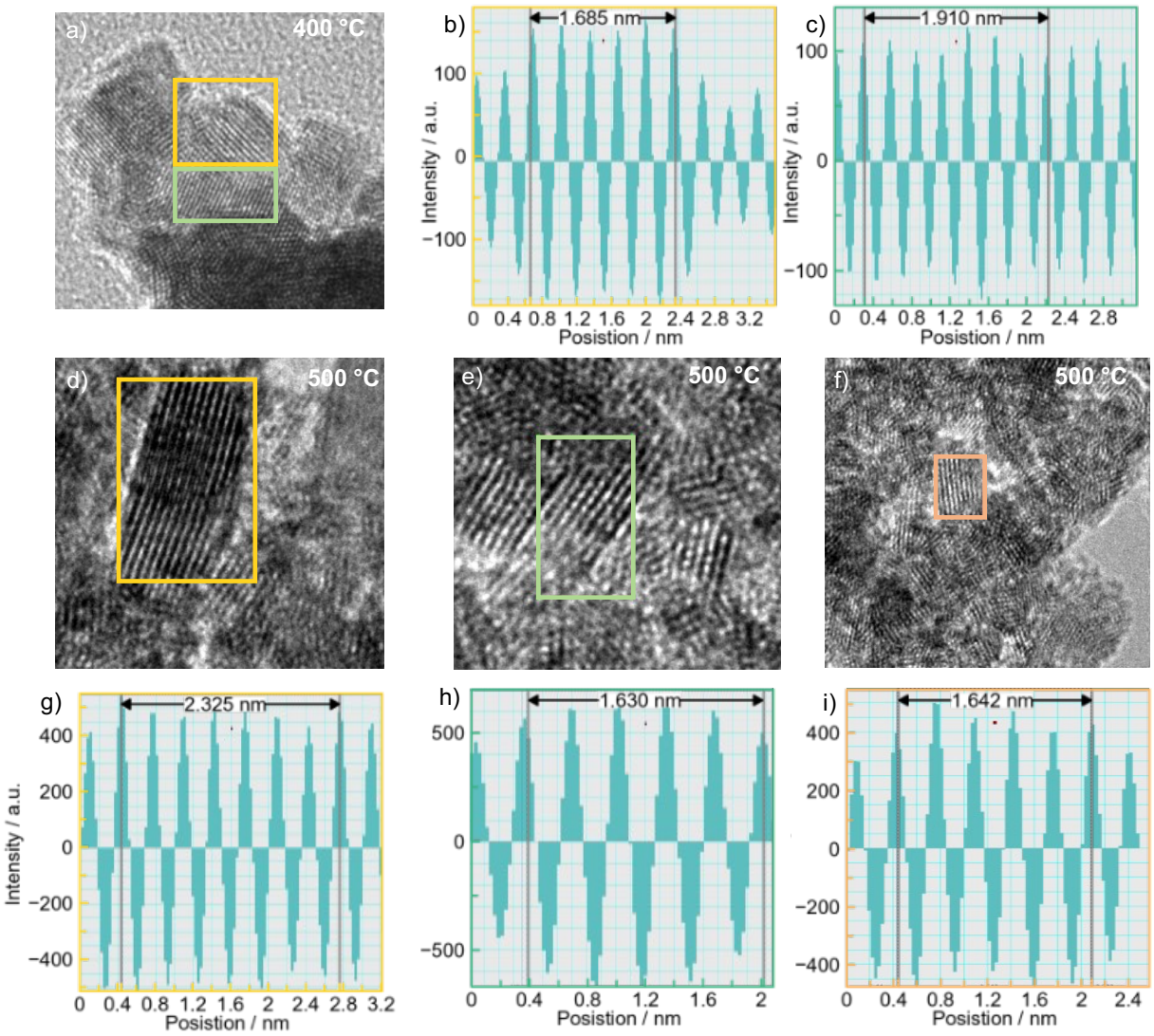

Figure S1. IFFT analysis of lattice fringes from TEM micrographs. a) 400 °C sample, with indications of the regions selected for IFFT analysis. b) IFFT of the yellow region in (a), yielding a d-spacing of 3.37 Å, corresponding to the (110)-crystallographic plane in rutile. c) IFFT of the green region in (a), yielding a d-spacing of 2.73 Å, corresponding to the (101)-crystallographic plane. d-f) TEM micrographs of the 500 °C sample with regions selected for IFFT analysis. g) IFFT of the yellow region in (d), yielding a d-spacing of 3.32 Å, corresponding to the (110)-crystallographic plane. h) IFFT of the green region in (e), yielding a d-spacing of 3.26 Å, corresponding to the (110)-crystallographic plane. i) IFFT of the orange region in (f), yielding a d-spacing of 3.28 Å, corresponding to the (110)-crystallographic plane.

Rietveld refinement of *ex situ* 500 °C sample

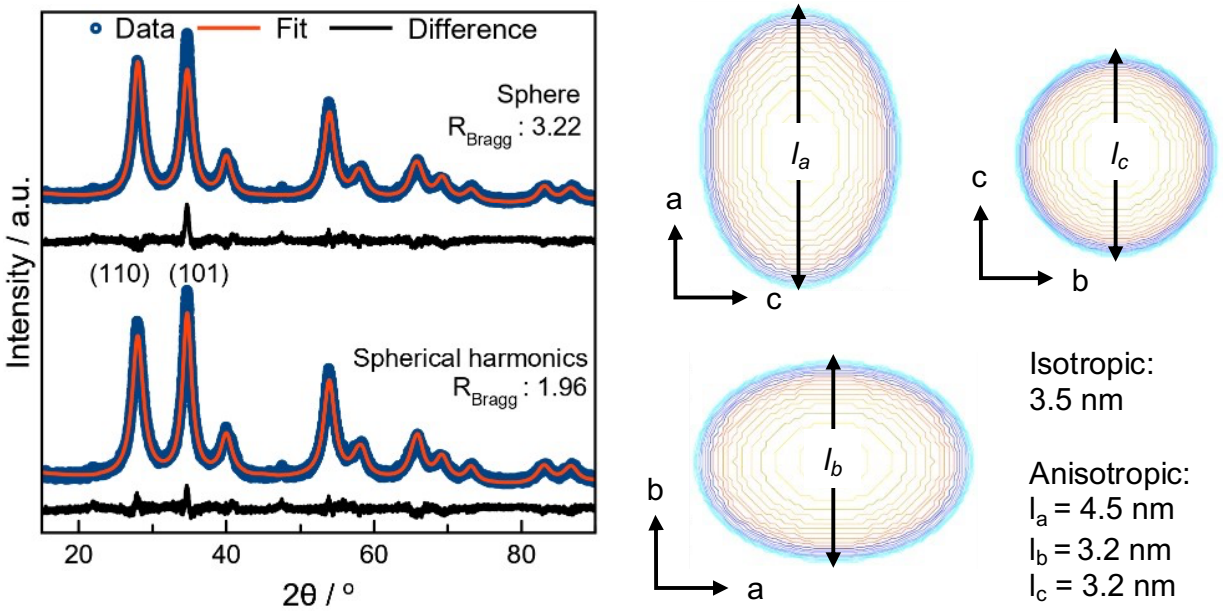

Figure S2. Left: Rietveld refinement of the IrO_2 sample annealed at 500 °C using two structural models. The first model assumes isotropic crystallite size (top), while the second incorporates an anisotropic crystallite elongation, modelled with a 2-term spherical harmonics function (bottom). The Y_{00} and Y_{20} parameters were refined in the anisotropic model. Right: Visualization of the anisotropic crystallite shape generated using the GFourier program within the FullProf Suite.[1] The crystallite dimensions along the Cartesian unit-cell axes were determined using the integral breadths from the refinement output of the (200) and (002) reflections.

Rietveld refinement of the 500 °C sample using a spherical rutile IrO_2 structural model confirms formation of IrO_2 (Figure S2 upper left). However, the intensity ratio of the (101) and (110) reflections is not well described by the spherical nanoparticle model. Specifically, the calculated intensity of the (101) reflection is significantly lower than the experimental data, suggesting preferential crystallite growth. To account for this suspected crystallite anisotropy, a two-term spherical harmonics model (Y_{00} and Y_{20}) is introduced, which greatly improves the fit (Figure S2, lower left). The crystallite dimensions were determined using the integral breadths of the (200) and (002) reflections from the Rietveld refinement. The refined crystallite shape (visualized in Figure S2 right) suggests elongated rod-shaped crystallites with a width of approximately 3.2 nm and a length of 4.5 nm have been formed.

Total scattering

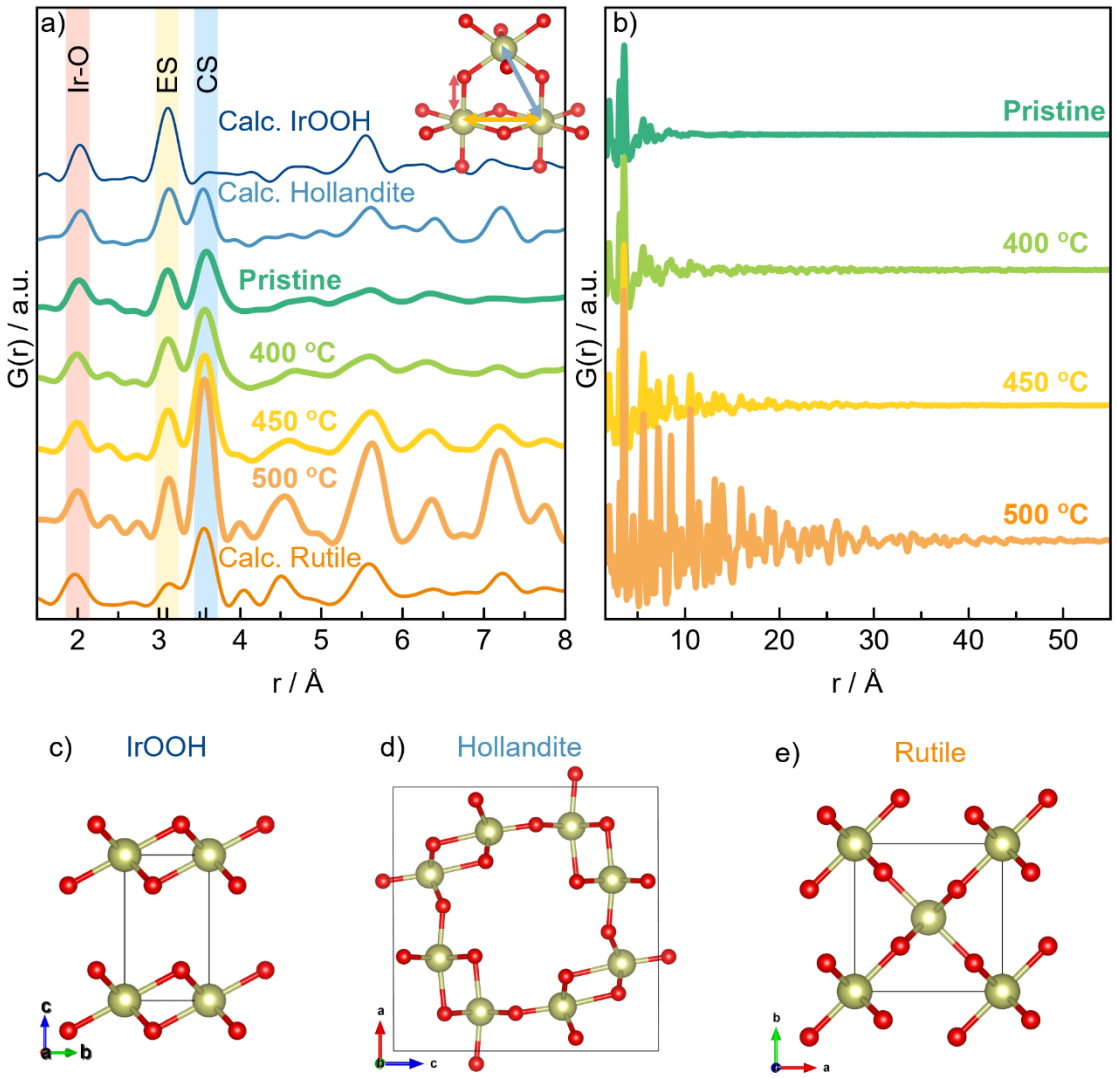

Figure S3. Comparison of the experimental PDFs in a) local region and b) full range, for the synthesized samples. Calculated PDFs of c) iridium oxyhydroxide (IrOOH, H removed for clarity), d) Hollandite IrO_2 ($K_{0.25}IrO_2$, K removed) and e) rutile IrO_2 are shown for comparison. The layered IrOOH structure consists exclusively of edge-sharing (ES) octahedra. Consequently, the absence of corner-sharing (CS) connectivity results in a CS peak intensity that does not match the experimental PDFs. In the hollandite structure, the peak intensities of the ES and CS Ir-Ir peaks are close to equal, whereas in the rutile structure, the CS peak is significantly more intense than the ES peak. Among the synthesized samples, the Pristine and 400 °C samples most closely resemble the local structure of hollandite-type IrO_2, while the 450 °C and 500 °C samples resemble the local structure of rutile.

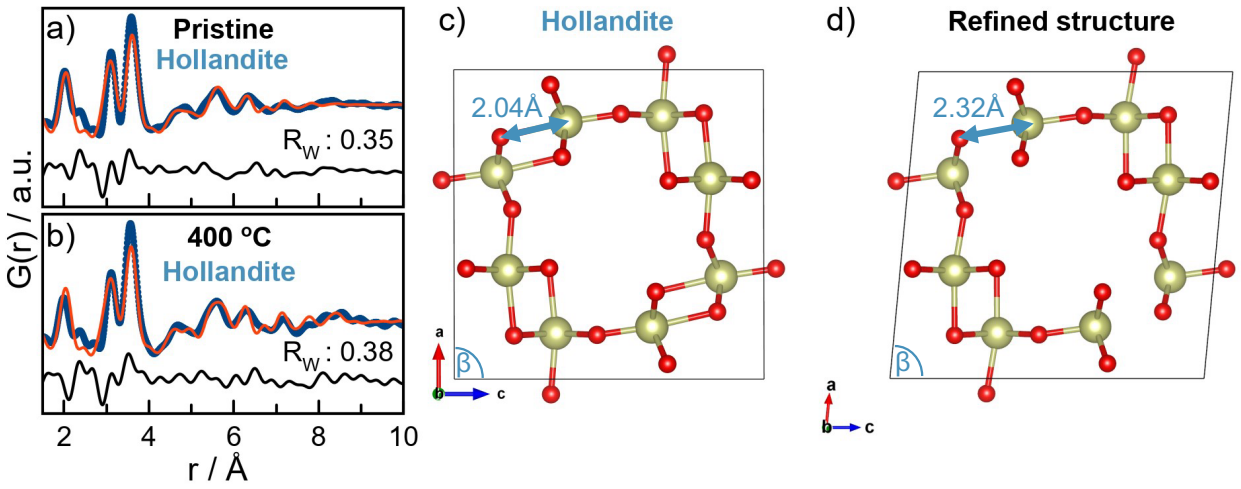

Figure S4. PDF fits to a) Pristine and b) 400 °C samples using K-removed hollandite IrO_2 as structural model. Fit parameters provided in Table 1S show decreased β angle, as evident when comparing the c) input structure and d) refined model (shown for the Pristine sample). Ir-O distances are in the refined models elongated to 2.32 Å, way above the longest reported Ir^{4+} bond length of 2.096 Å.[2]

Table S1. PDF refinement parameters obtained from fits shown in Figure S4. Modifying a hollandite structure ($K_{0.25}IrO_2$) to remove K provides the IrO_2 hollandite model used for fitting. A spherical envelope function is employed. The data were fitted in a range of 1.5-15 Å with δ_2 = 2.0 Å^2. Fit parameters include scale factor, lattice parameters, and spherical size.

Model	IrO_2 Hollandite					
Sample	Pristine			400 °C		
Scale factor	1.35325			1.45643		
Cell parameters [Å] and angle [º]	a=10.2658	b=3.1323 β=84.619	c=10.4896	a=10.1365	b=3.1349 β=84.765	c=10.4271
U_{iso} [Å^2]	M=0.005	O=0.005		M=0.005	O=0.005	
Crystal diameter [Å]	9.02			10.3		
R_w	0.35			0.38		

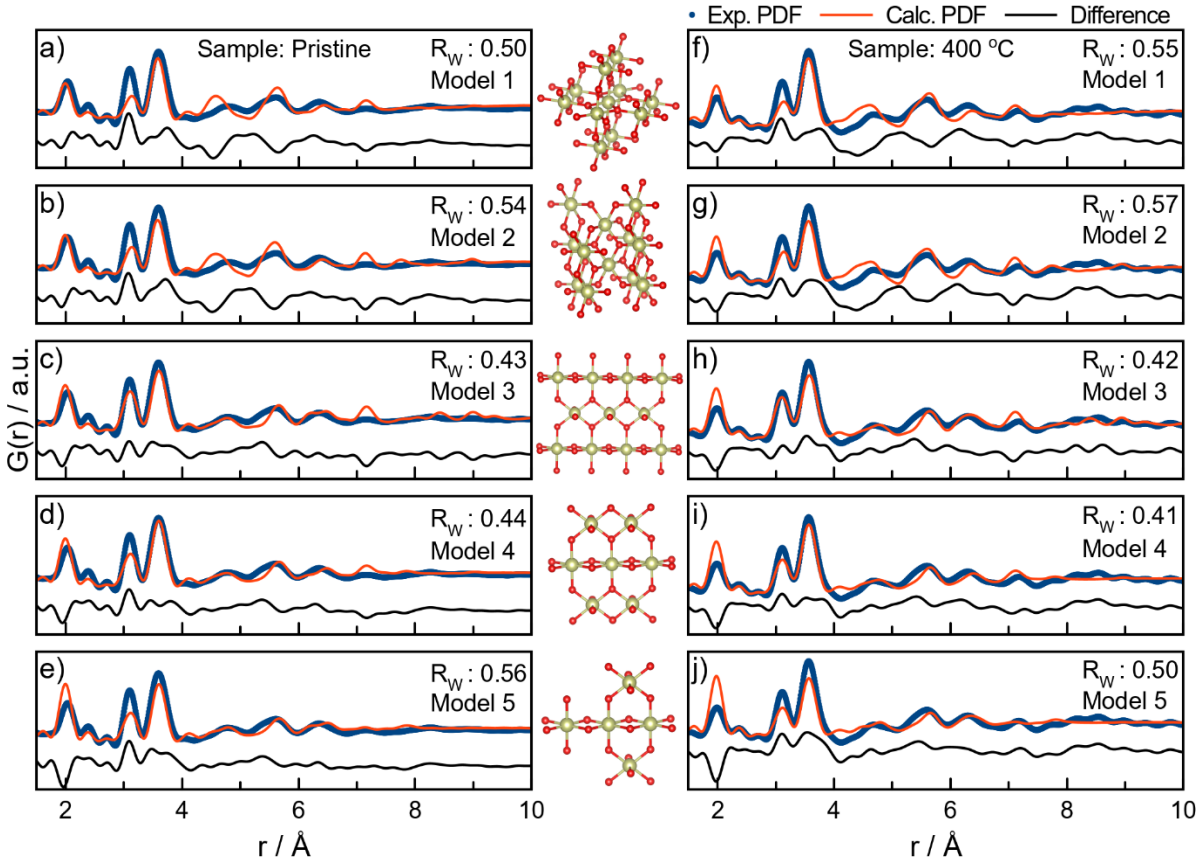

Figure S5. PDF fits using structural motifs cut out from rutile IrO_2. a-e) Fitted to PDF data obtained from the Pristine sample. f-j) Fitted PDF data measured on the 400 °C sample.

The spherical and elongated IrO_x clusters (Models 1 and 2) fail to describe the 3.1 Å peak intensity and the PDF features beyond 4 Å (Figure S5a-b, f-g). In contrast, the sheet-like motifs (Models 3-5) provide a much better fit for both samples in the range above 4 Å (Figure S5c-e, h-j). However, the smallest sheet, "Model 5" (Figure S5e, j), overestimates the Ir-O peak (2.0 Å) and underrepresents the ES and CS Ir-Ir peaks (3.1 Å and 3.56 Å), suggesting it is too small to represent the actual particles. Based on the goodness-of-fit (R_W-value), Models 3 and 4 do an equally good job of describing the Pristine (Figure S5c-d) and 400 °C (Figure S5h-i) PDFs. The three peaks between 4.5 Å and 7.5 Å are well described by either model. Both consist of edge-sharing [IrO_6]-octahedra linked through corner-sharing to form sheets cut from the rutile (110)-plane.

Small-angle X-ray scattering

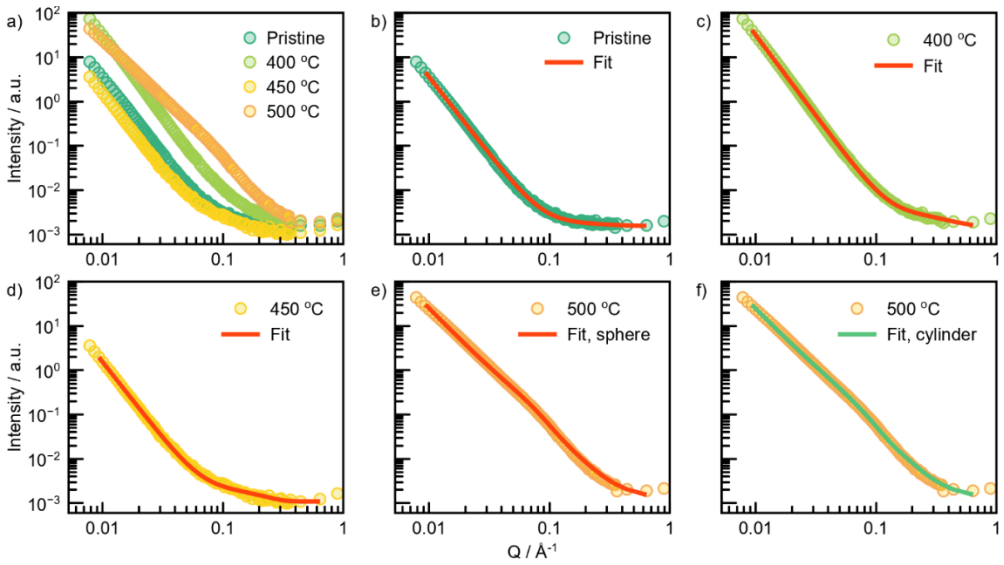

Figure S6. a) Overview of SAXS curves collected for the *ex situ* hydrothermally synthesized Pristine sample and after annealing at 400 °C, 450 °C, and 500 °C. Fit of spherical particles from b) Pristine, c) 400 °C, d) 450 °C, e) 500 °C samples. f) 500 °C sample fitted using a cylindrical form factor. The fit variables are listed in Table S2.

SAXS measurements were performed on the four IrO_x samples (Figure S6a). The SAXS data were corrected for solvent and capillary background, log-binned, and fitted using a spherical (and cylindrical for the 500 °C sample) form factor and power law. Polydispersity was modelled using the Schulz-Zimm distribution. SAXS fits are shown in Figure S6b-f with corresponding number weighted fit parameters listed in Table S2. Spherical diameters of 1.2 nm, 1.2 nm, and 2.2 nm were obtained for the Pristine, 400 °C, and 450 °C samples, respectively. Due to the high noise-to-signal ratio in the Q-range of 0.2-0.4 Å^{-1} and the low scattering intensity of the small nanoparticles, it was not possible to determine the polydispersity of the Pristine, 400 °C, and 450 °C samples. The high noise in this Q-range arises from merging the signals from the Nano-inXider instrument's WAXS and SAXS detectors, where the coverage of this Q-region is incomplete, leading to reduced counting statistics. For the 500 °C sample, the fit below Q = 0.1 Å^{-1} is slightly improved when changing from a spherical form factor (Figure S6e) to a cylindrical one (Figure S6f).

Table S2. Fit parameters obtained from fitting a model of a sphere or elongated rod to the SAXS data measured on *ex situ* synthesized IrO_x, shown in Figure S6.

IrO_x sample	**Scale**	**Radius / Å**	**Poly-dispersity**	**Scale powerlaw**	**Power**	**Background**
Pristine	1.64E-3	7	0	3.9E-7	3.48	1.6E-3
Annealed 400 °C	18.83E-3	6	0	1.70E-6	3.64	1.6E-3
Annealed 450 °C	2.00E-3	11	0	1.8E-7	3.46	1.1E-3
Annealed 500 °C (spherical model)	11.20E-3	25	0.3	8.1E-5	2.74	1.3E-3
Annealed 500 °C (cylindrical model)	14.26E-3	25 (radius)	0.2	6.7E-5	2.77	1.4E-3
		147 (length)	0.2			

Operando gas diffusion electrode (GDE) setup

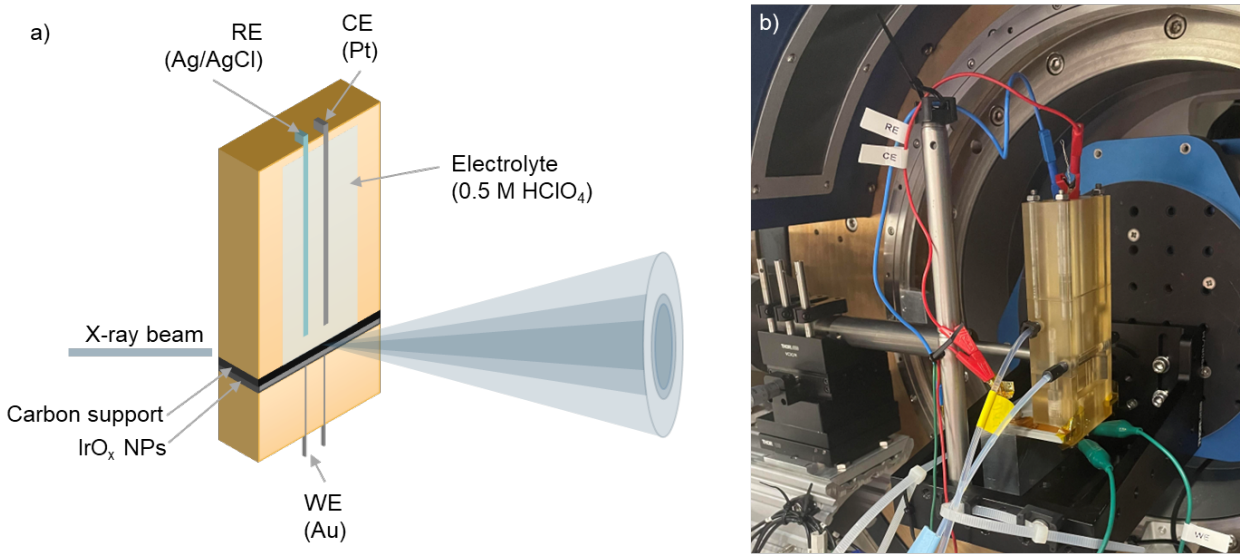

Figure S7. a) Schematic of the *operando* gas diffusion electrode (GDE) cell used for total scattering measurements during OER conditions. b) Photograph showing the *operando* cell setup installed at the 15-1 beamline at Diamond Light Source. IrO_x particles, synthesized in our lab, were vacuum filtrated onto a carbon gas diffusion layer (GDL). The IrO_x catalyst, supported on carbon, is mounted in the *operando* cell. A 0.5 M $HClO_4$ solution is continuously pumped through the cell while total scattering data is collected.

Operando PDF compared to *ex situ*

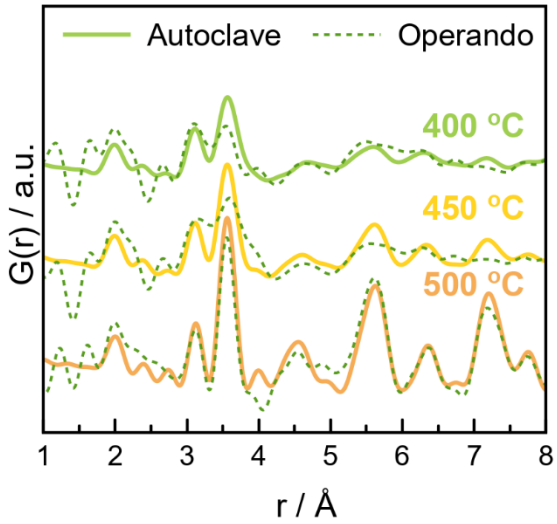

Figure S8. PDF comparison of as-synthesized IrO_x NPs (bold line) with NPs deposited on a carbon support and measured in the electrochemical cell (dashed line).

Comparison of unsupported NPs measured *ex situ* and carbon gas diffusion layer supported NPs measured in the electrochemical cell without electrolyte. We note deviations between the two setups. The peak positions are similar between the measurements; however, an intensity deviation exists. Furthermore, a negative peak at 1.4 Å and 2.4 Å is observed in the *operando* measurement for the 400 °C and 450 °C samples. As observed in Figure S9, the peak stems from a slight over-subtraction of the background carbon peak.

Background subtraction of *operando* PDF

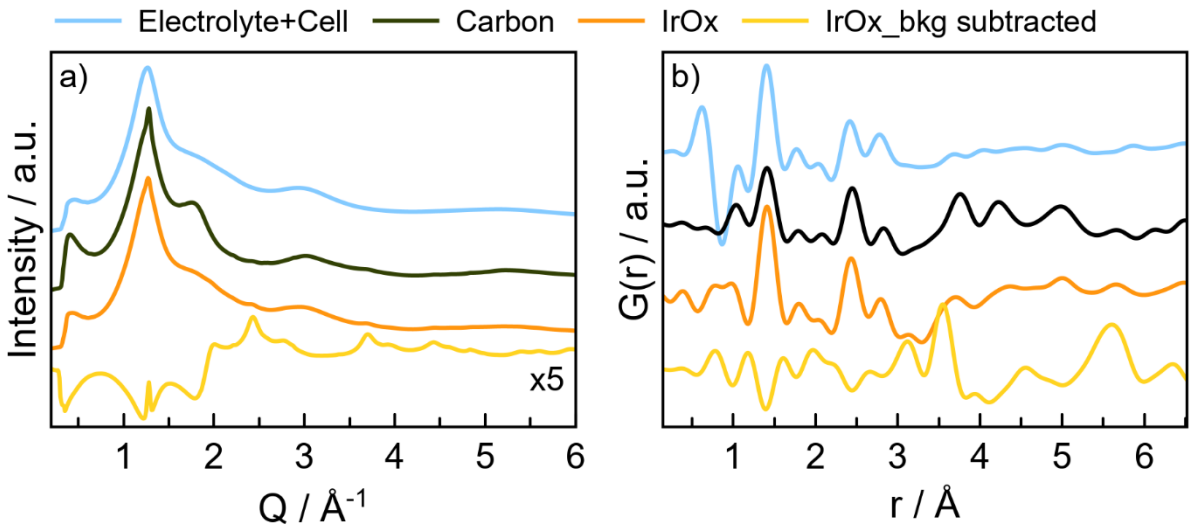

Figure S9. Background and sample measurements. Electrolyte in the electrochemical cell is plotted in blue, with the carbon diffusion layer in the electrochemical cell in black. The orange graph corresponds to the measurement of the IrO_x 500 °C sample deposited on a carbon diffusion layer in the operating electrochemical cell at 1.6 V_{RHE} potential. The yellow graph is the result of the linear combination subtraction of the background components from the PXRD corresponding to the orange graph. a) XRD. b) PDF.

Performing *operando* X-ray total scattering experiments introduces experimental challenges, particularly with detector alignment, as even slight deviations can affect data quality given the proximity needed for high-Q measurements. Lacking an internal standard introduces uncertainties, and background subtraction requires precise measurements of each component's scattering signal (electrolyte, catalyst support, and cell materials). Background changes, such as those from dissolution or bubble formation, further complicate this process, reducing scattering data quality compared to traditional capillary setups.

In this study, the *operando* PDF measurements were performed in an electrocatalytic cell with liquid 0.5 M $HClO_4$ electrolyte. The IrO_x sample was deposited on a carbon gas diffusion layer. Hence, backgrounds were measured on the electrocatalytic cell with electrolyte, and on a blank carbon gas diffusion layer within the empty electrocatalytic cell. Background subtraction was performed using a linear combination analysis to find the correct scaling between the "electrolyte in cell" (blue graph in Figure S9a) and "carbon in cell" (black graph in Figure S9a) components. The structural complexity of the carbon layer, comprising both gas diffusion and mesoporous layers, results in uneven scattering contributions, which cause an over-subtraction of background at Q-values below 2 $Å^{-1}$. However, at higher Q-values, where the total scattering data is most critical, the background subtraction is successfully handled, ensuring PDFs of adequate quality.

Electrochemical response of *operando* OER

The open circuit potentials (OCP) of the IrO_x catalysts are tabulated in Table S3, while the electrochemical response for the measurements is shown in Figure S10.

Table S3. Open circuit potentials (OCP) measured of the three IrO_x catalyst samples in 0.5 M perchloric acid electrolyte solution.

IrO_x samples	OCP / V_{RHE}
Annealed 400 °C	0.499
Annealed 450 °C	0.397
Annealed 500 °C	0.442

***Operando* PDFs**

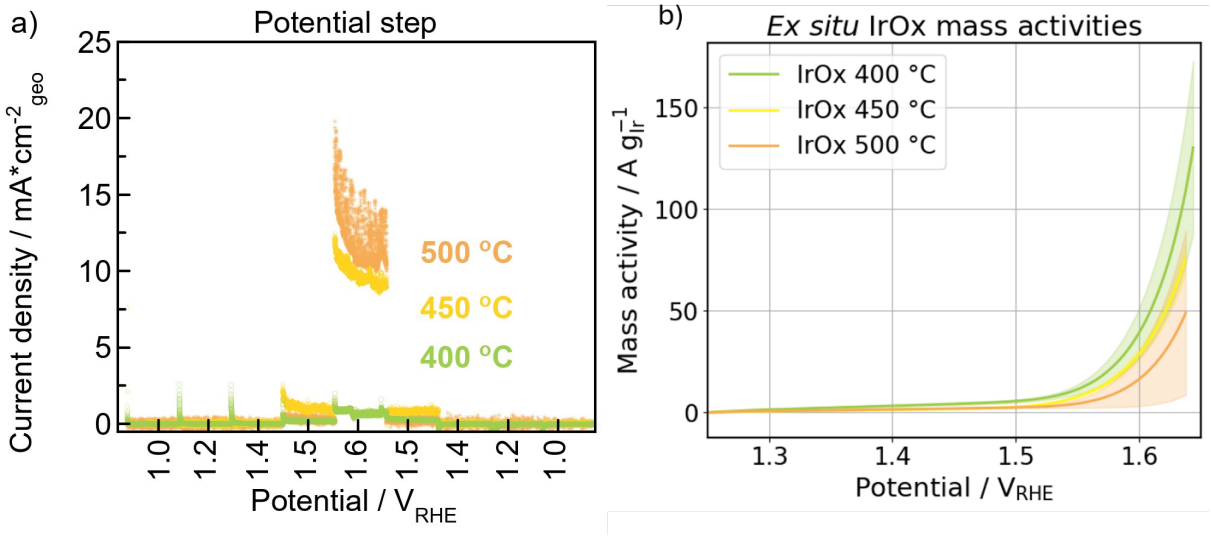

Figure S10. a) Electrochemical response during potential step protocol. The electrochemical responses have been normalized to the geometric surface area of 0.2572 cm^2. b) *Ex situ* OER activity measurements conducted on a multiworking electrode containing eight individual electrodes per sample. The data is iR and capacitance corrected. The uncertainties shown are 95 % confidence intervals calculated based on Student's t-test. CVs recorded in 0.5 M H_2SO_4 electrolyte at 0.01 V s^{-1}. The 10th scans are shown. Further experimental details are found in the experimental methods section.

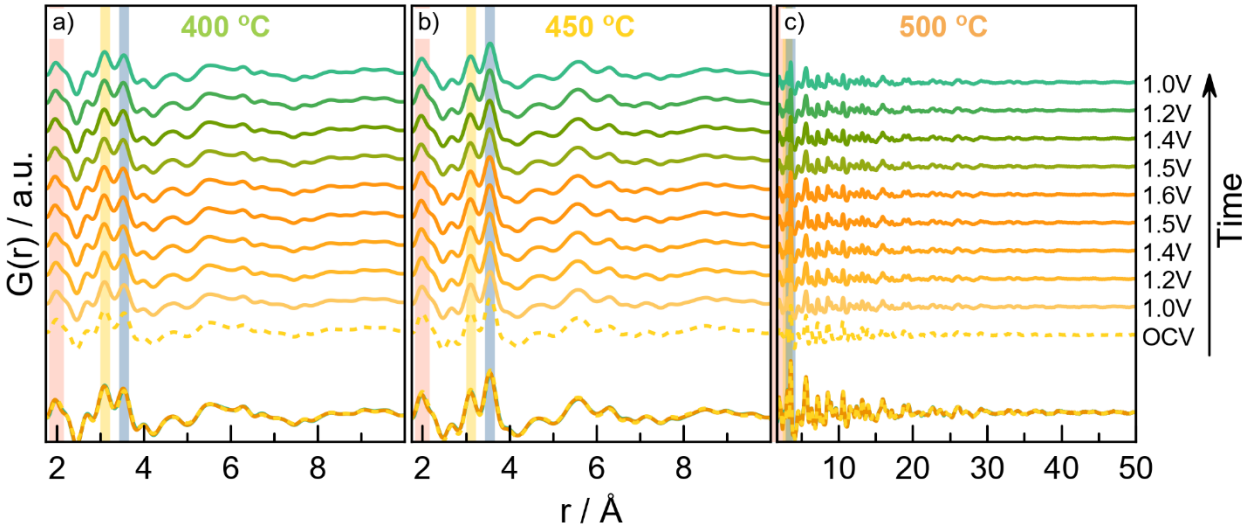

Figure S11. Extended *r*-range of the PDFs collected during *operando* chronoamperometry step protocol (shown in Figure 7), stepping from OCP to 1.6 V_{RHE} and back to 1.0 V_{RHE}. a) 400 °C sample, b) 450 °C sample, and c) 500 °C sample.

Gaussian fitting of *operando* PDFs

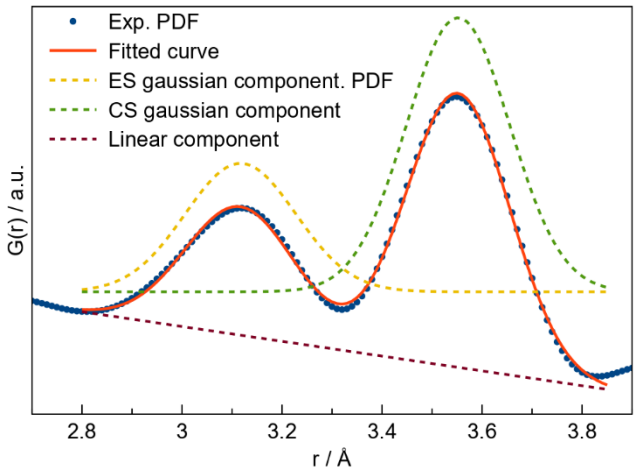

Figure S12. We here illustrate the procedure used for the Gaussian fitting applied to extract peak positions and peak intensity ratios from PDF data. This figure provides an example using the PDF obtained on the 500 °C sample during *operando* total scattering at a potential hold of 1.6 V_{RHE}. The fitted Gaussian curve, shown in red, consists of three components: a Gaussian representing each peak, with edge-sharing Ir-Ir bonds indicated by the dashed yellow line and corner-sharing Ir-Ir bonds indicated by the dashed green line. Additionally, a linear component (dashed brown) is included to account for the underlying background. This fitting procedure was consistently applied throughout the analysis; however, for the Ir-O peak, only a single Gaussian and a linear component were used.

***Operando* stability measurements with potential hold**

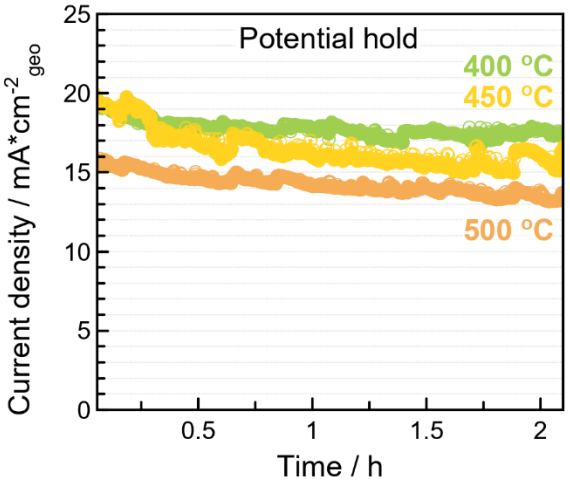

Figure S13. Electrochemical response during chronoamperometry at 1.65 $V_{RHE.}$ The electrochemical responses have been normalized to the geometric surface area of 0.2572 cm^2. Fluctuations are observed during the 2-hour test, which are attributed to bubble formation blocking the catalytic surface, which later detaches again.

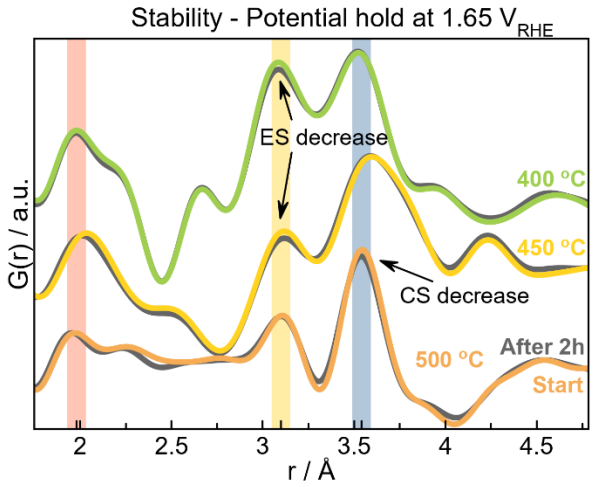

Figure S14. PDF before (colored line) and after (grey line) potential hold at 1.65 V_{RHE} is performed. Significant distances are highlighted: Ir-O in red, ES Ir-Ir in yellow, CS Ir-Ir in blue.

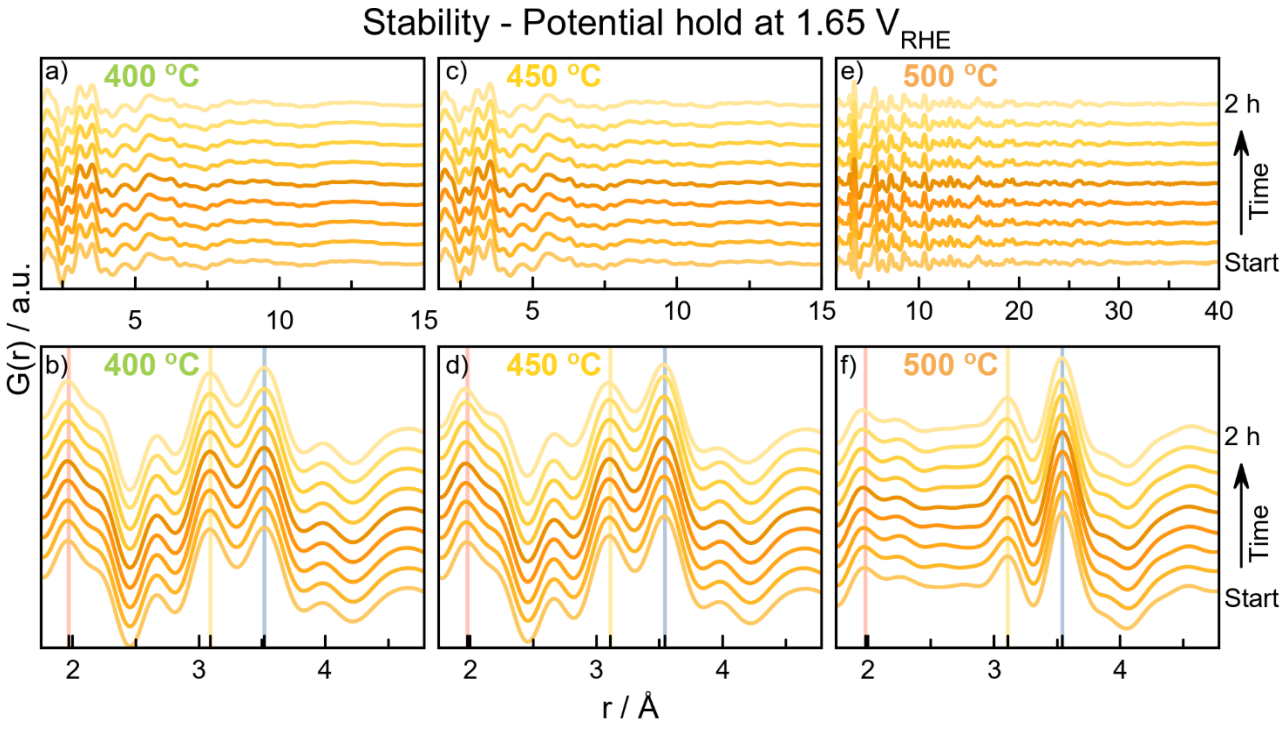

Figure S15. PDF during chronoamperometry at 1.65 V_{RHE}. a-b) 400 °C sample. c-d) 450 °C sample. e-f) 500 °C sample.

Post-mortem (S)TEM

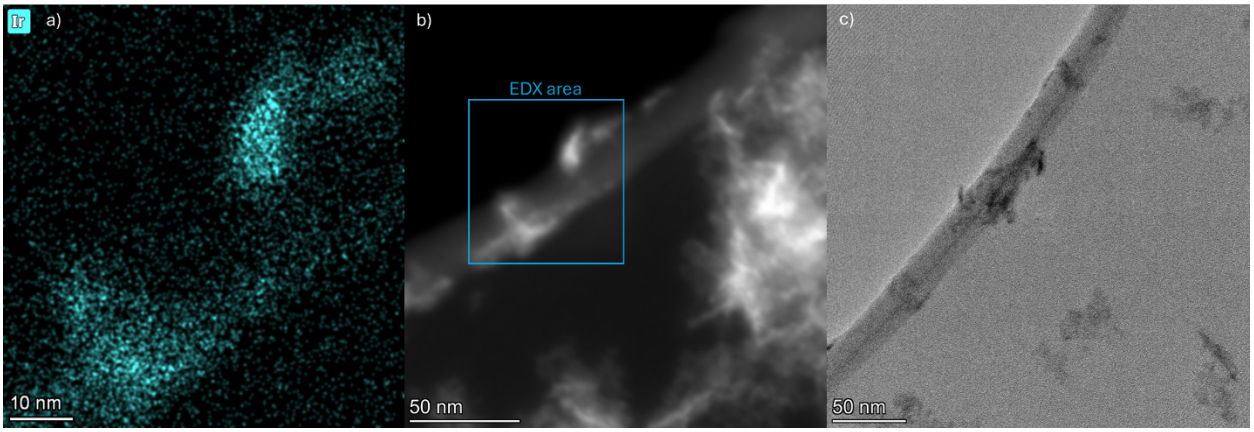

Figure S16. Post-mortem STEM-EDX and TEM on the 500 °C sample after stability test. a) Ir elemental mapping with b) corresponding HAADF-STEM. The EDX area is highlighted in blue. c) TEM showing elongated morphology of the IrO_x particles.

References

1. J. Rodríguez-Carvajal, Recent advances in magnetic structure determination by neutron powder diffraction, *Physica B*, 1993, **192**, 55-69.
2. O. C. Gagne and F. C. Hawthorne, Bond-length distributions for ions bonded to oxygen: results for the transition metals and quantification of the factors underlying bond-length variation in inorganic solids, *IUCrJ*, 2020, **7**, 581-629.